materials

MDPI

Article

Investigation of the Effect of Volumetric Hydrophobization on the Kinetics of Mass Transfer Processes Occurring in Cement Concretes during Corrosion

Viktoriya S. Konovalova

Department of Natural Sciences and Technosphere Safety, Ivanovo State Polytechnic University, Sheremetevsky Ave., 21, Ivanovo 153000, Russia; kotprotiv@yandex.ru

Abstract: The entry of aggressive substances into the pore structure of concrete causes the development of corrosion processes and leads to the destruction of the cement stone structure. Hydrophobic additives provide high density and low permeability and are an effective barrier to the penetration of aggressive substances into the structure of cement stone. To assess the contribution of hydrophobization to the durability of the structure, it is necessary to know how much the processes of corrosive mass transfer slow down. To study the properties, structure and composition of the materials studied in the work (solid and liquid phases) before and after exposure to liquid-aggressive media, experimental studies were carried out using chemical and physicochemical analysis methods: determination of density, water absorption, porosity, water absorption and strength of cement stone; differential thermal analysis; quantitative analysis of calcium cations in liquid medium by complexometric titration. The article presents the results of studies of the effect on the operational characteristics of the introduction of a hydrophobic additive of calcium stearate into the cement mixture at the stage of concrete production. The effectiveness of volumetric hydrophobization was evaluated to prevent the penetration of an aggressive chloride-containing medium into the pore structure of concrete destruction and the leaching of calcium-containing components of cement stone. It was found that the introduction of calcium stearate in an amount of 0.8–1.3% by weight of cement increases the service life of a concrete product during corrosion in liquid chloride-containing media with a high degree of aggressiveness by four times.

Keywords: volumetric hydrophobization; corrosive mass transfer; concrete corrosion; corrosion kinetics; hydrophobizing additive; hydrophobized concrete; waterproof concrete

check for updates

Citation: Konovalova, V.S. Investigation of the Effect of Volumetric Hydrophobization on the Kinetics of Mass Transfer Processes Occurring in Cement Concretes during Corrosion. *Materials* **2023**, *16*, 3827. https://doi.org/10.3390/ma16103827

Academic Editor: Lizhi Sun

Received: 12 March 2023
Revised: 4 May 2023
Accepted: 17 May 2023
Published: 18 May 2023

Copyright: © 2023 by the author. Licensee MDPI, Basel, Switzerland. This article is an open access article distributed under the terms and conditions of the Creative Commons Attribution (CC BY) license (https://creativecommons.org/licenses/by/4.0/).

1. Introduction

During the operation of concrete, various aggressive substances affect it, which leads to a decrease in its durability. The durability assessment is related to the expected performance characteristics of the product and consists in determining the factors that are crucial for the destruction of the material depending on its composition and properties, determining changes caused by the interaction of the material with external-aggressive media, and measuring damage over time.

The main physicochemical processes of destruction in reinforced concrete products occur due to the penetration of water into the concrete structure [1–5]. The penetration of water into the pores occurs by various mechanisms and is determined by the degree of saturation of concrete. The microstructure of concrete has a great influence on the rate of water penetration. When unsaturated concrete is exposed to an aqueous environment, even in the absence of pressure, water will be absorbed into the pore structure due to capillary suction [6,7].

In order to prevent and reduce the penetration of water and dissolved aggressive substances into the pore structure of concrete, its hydrophobization is ensured. The purpose

of volumetric hydrophobization is to compact concrete to prevent water ingress and/or to make the capillary surface non-wettable, which will eventually reduce water penetration.

Special additives are used to create waterproof concrete. They reduce the probability of water ingress, reducing the permeability and shrinkage of concrete during drying [8]. Additives are introduced into the water-cement mixture in small quantities to increase the durability of concrete, improve its properties, and control setting or hardening [9–11]. It can be liquid or powdery substances. Hydrophobizing additives differ in chemical basis depending on the type of concrete, cement mortar, or plaster [12].

Hydrophobic additives introduced into concrete usually act on the basis of one or a combination of three mechanisms: reduction of capillarity by reducing the water–cement ratio, hydrophobization of capillaries, and physical or chemical blocking of pores. Reactive silicates [13,14], calcined clays [15,16], colloidal silicon dioxide [17,18], lignosulfonates [19], naphthalene sulfonate formaldehyde [20–22], sulfated melamine formaldehyde [22,23], and polycarboxylate ether [24–26] are used to reduce the capillarity of concrete. Hydrophobization of capillaries is achieved by introducing into concrete soap [27], bitumen [28], mineral oils [29,30], fatty acids [31], calcium and zinc stearates [32–35], butyl stearate [36,37], acrylic resins [38,39], thin wax emulsions [40,41], silicones [42,43], silane-siloxanes [44,45]. For example, stearates react chemically with calcium hydroxide in cement, resulting in the formation of a layer of insoluble calcium stearate on the walls of the pores of cement stone, providing water repellency [46]. Physical pore blocking can be achieved with the help of inert powder fillers such as talc [47], bentonite [48] or with the help of fine waxes [49], bitumen [50], acrylic emulsions [51], and emulsion styrene–butadiene rubbers [52,53]. Chemical pore blocking is carried out using microfine latent hydraulic reactive silicates [54] or pozzolan nanoparticles [55,56], providing secondary hydration to achieve the most dense packing of C-S-H gel in a cement matrix at the nanoscale. In the above materials, available free lime $Ca(OH)_2$ is used for recrystallization and formation of new, more stable C-S-H and C-A-S-H phases in the presence of water [57]. These materials used as additives are also called crystal additives.

The positive effect of concrete hydrophobization usually lies in the fact that this type of treatment prolongs the period before the onset of corrosion. When corrosion begins, the hydrophobicity of the surface of the pores of the cement stone effectively prevents the penetration of the liquid medium and reduces the rate of corrosion processes [58]. When examining the motorway pier after seven years of operation, no chlorides were found in the hydrophobized concrete [59]. Hydrophobic additives do not have a negative effect on the strength of concrete; on the contrary, some concretes with hydrophobic additives have increased strength [9,60]. Since water-repellent substances are evenly distributed over the entire volume of concrete, they do not change the appearance of the product. In addition, hydrophobic additives are effective for reducing efflorescence since the migration of water throughout the entire volume of concrete is reduced [61,62].

In individual and mass construction of structures operated under the influence of liquid media, the use of concrete grades for water resistance W10–W16 is widespread. The corrosion resistance of reinforced concrete with hydrophobic additives in a highly aggressive chloride-containing environment needs additional research. In order to assess the contribution of hydrophobization to the durability of a concrete structure, it is necessary to know how effectively this treatment method prevents the penetration of various aggressive substances into the structure of cement stone and how long this efficiency can be maintained.

2. Materials and Methods

2.1. Materials

For the production of cement stone samples, Portland cement with a standardized composition without mineral additives of the CEM I 42.5 N brand was used as a binder. The choice of this brand of Portland cement is due to its prevalence and demand in mass

construction. The chemical and mineralogical composition of Portland cement of the CEM I 42.5 N grade, established by the quality certificate, are presented in Tables 1 and 2.

Table 1. Chemical composition of Portland cement CEM I 42.5 N.

Components	SiO_2	Al_2O_3	Fe_2O_3	CaO	MgO	SO_3	R_2O
Amount [%]	21.24	5.65	4.30	65.87	0.86	0.44	0.71

Table 2. Mineralogical composition of Portland cement CEM I 42.5 N.

Components	C_3S	C_2S	C_3A	C_3AF
Amount [%]	61.40	14.60	7.69	13.01

Cement stone samples were made from solutions of normal density with a water–cement ratio W/C = 0.3. The tests were carried out after 28-day hardening of the samples at a temperature of 20 ± 2 °C and relative humidity of 50–70%. Corrosion studies were carried out on cubic samples of cement stone with a face of 3 cm. The cement stone was placed for 150 days in containers filled with a 2% $MgCl_2$ solution. The choice of a 2% $MgCl_2$ solution for corrosion tests is due to the high activity of chloride ions that create an aggressive environment for concrete [63]. The solutions were prepared and operated at a temperature of 20 °C.

The grade of cement for water resistance was regulated by a hydrophobic additive calcium stearate and, before the experiment, was determined by the method described in Section 2.2. Calcium stearate was introduced into the cement mixture at the stage of sample production to ensure volumetric hydrophobization. It was experimentally found that the grade of concrete W10 corresponds to the concentration of the hydrophobizer in the amount of 0.8% by weight of cement, grade of concrete W14–1.1%, and grade of concrete W16–1.3%. The characteristics of cement stone samples with calcium stearate additives are presented in Table 3.

Table 3. Characteristics of hydrophobized cement stone.

Characteristic	Concrete Grade for Water Resistance		
	W10	W14	W16
Density [kg/m^3]	2432.1	2568.2	2604.4
Water absorption [%]	4.0	3.7	3.5
Porosity [%]	6.8	6.0	5.7
Strength [MPa]	54.58	58.18	63.39

Each type of test described below in this section was performed on a series of five cement stone samples. The results in the article are given for average values.

2.2. Method of Determining the Grade of Concrete by Water Resistance

The grade of concrete for water resistance was determined according to the method described in the patent [64] and MI 2625-2000 «Recommended Practice—National Measurement Standards—Cement Materials—Accelerated Method for Measuring Water Impermeability» [65]. After drying at a temperature of 105 ± 5 °C to a constant mass, the cement samples under study were split into two parts, after which paraffin waterproofing was applied to the side surfaces. Then, samples were saturated with water through the split surface in 1 and 5 min, respectively, and the equivalent capillary pressure in the material was found depending on the capillary porosity of the material and the volume of absorbed water. An indicator of the degree of the kinetics of water saturation was established, the

volume of capillary pores of the mortar part of the material was determined, and the water resistance of cement materials was calculated by the formula:

$$\lambda' = \left(\frac{P_i}{0.2}\right)^n \cdot \sqrt{1 + \frac{P_i}{P_C}}, \quad (1)$$

where P_i is definable water resistance [MPa], P_C is equivalent capillary pressure resulting from water saturation of materials [MPa], and n is the indicator of the degree of the kinetics of water saturation of the material, determined by the formula:

$$n = \frac{lg\Delta\overline{m}_5 - lg\Delta\overline{m}_1}{0.7}, \quad (2)$$

where $\Delta\overline{m}_1$ and $\Delta\overline{m}_5$ are arithmetic mean values of the mass difference of water-saturated and dried samples for 1 and 5 min, respectively; λ is the criterion determined by the formula:

$$\lambda = \frac{V_{Ci}}{(\tau')^n \Delta V_{C1}}, \quad (3)$$

where V_{Ci} is the volume of capillary pores of the material in the test sample, [cm^3]; ΔV_{C1} is the volume of water absorbed by the capillaries of the material in 1 min, [cm^3]; τ' is relative reduced time, depending on the size and shape of the tested samples (from MI 2625-2000).

The value of ΔV_{C1} is calculated by the formula:

$$\Delta V_{C_1} = \frac{\Delta\overline{m}_1}{\gamma_L} \cdot \left(1 - \frac{K_6 \cdot \Delta V' C}{W - \beta_1 S - \beta_2 L - K_3 \Delta V' C}\right), \quad (4)$$

where W is the volume of the mixing water in 1 L of the compacted mixture of the material, [cm^3]; S, L are the content by weight of fillers in 1 L of a compacted mixture of material, respectively small and large, [g]; β_1, β_2 are water absorption of aggregates in fractions of their mass during mixing and compaction of the mixture, respectively, small and large, [cm^3/g]; K_3, K_6 are coefficients from MI 2625-2000; $\Delta V'$ is the specific current contraction of the cement used at the time of testing the material ($\Delta V'$ = 2486 cm^3/g); C is the content by weight of cement in 1 L of compacted mixture, [g].

The equivalent capillary pressure P_C is calculated by the formula:

$$P_C = \frac{A_1 \cdot p_{cap}^2}{M \cdot \Delta V_{C_1}^2 \cdot f^2}, \quad (5)$$

where A_1 is constant from in MI 2625-2000; f is the coefficient reflecting the ratio of the volume of concrete to the volume of its mortar part; M_1 is the parameter that integrally reflects the features of the capillary structure and the «overflow» effect is calculated by the formulas:

- for concrete with a large aggregate: $M = 6 + 300 p_{cap}^{3/2}$;
- for fine-grained concrete: $M = 12 + 540 p_{cap}^{3/2}$.

The volume of capillary pores in the material of the tested concrete sample is determined by the formula:

$$V_C = \frac{V \cdot p_{cap}}{f}, \quad (6)$$

where V is the volume of the test sample, [cm^3].

The coefficient f is determined by the formula:

$$f = \frac{1000\gamma_L}{1000\gamma_L - L}. \quad (7)$$

The capillary porosity of the solution part is determined by the formula:

$$p_{cap} = \frac{W - \beta_1 S - \beta_2 L - K_5 \Delta V' C}{1000 - \frac{L}{\gamma_L}}, \quad (8)$$

where γ_L is the true density of coarse aggregate, [g/cm^3]; K_5 is the stoichiometric constant from MI 2625-2000.

The tested sample was assigned a water resistance mark equal to the lower closest to P_i value W given in GOST 12730.5-2018 «Concretes. Methods for determination of water tightness» [66].

2.3. Determination of Density, Water Absorption, and Porosity of Concrete

Concrete density is defined as the ratio of the mass of concrete (sample) in a state of natural humidity to its total volume. The volume of samples of the correct shape is calculated by their geometric dimensions. The dimensions of the samples are determined by a ruler or a caliper with an error of no more than 1%. The mass of the samples is determined with an error of no more than 0.1%.

The density of concrete ρ_c is calculated by the formula:

$$\rho_c = \frac{m}{V} \cdot 1000, \quad (9)$$

where m is sample weight, [g] and V is sample volume, [cm^3].

The true density of concrete is determined by measuring the mass of the unit volume of the crushed and dried sample. The initial sample is crushed in a laboratory crusher to a size of less than 5 mm, mixed, and reduced to 150 g. The resulting sample is again crushed to a size of less than 1.25 mm, mixed, and reduced to 30 g. Then it is crushed in a mortar to a powdery state (less than 0.125 mm), dried to a constant mass, cooled to room temperature, and two samples of 10 g each are weighed.

Each sample is poured into a clean, dry pycnometer, where distilled water at room temperature is poured in such an amount that the pycnometer is filled with no more than half of its volume. The pycnometer is placed in a slightly inclined position on a sand or water bath; its contents are boiled for 20 min to remove air bubbles. After removing the air, the pycnometer is wiped, cooled to room temperature, filled to the mark with distilled water, and weighed. Then the pycnometer is released from the contents, washed, filled to the mark with distilled water at room temperature, and weighed.

The true density of concrete ρ is calculated by the formula:

$$\rho = \frac{m \cdot \rho_w}{m + m_1 - m_2}, \quad (10)$$

where m is the mass of the crushed sample, [kg], ρ_w is water density, [kg/m^3], m_1 is the weight of a pycnometer with distilled water, [kg], and m_2 is the mass of the pycnometer with a sample and distilled water, [kg].

Water absorption is determined by testing a series of samples with dimensions $10 \times 10 \times 10$ cm. The samples are placed in a container filled with water at a temperature of 20 ± 2 °C above the upper level of the stacked samples by about 50 mm. Samples are weighed every 24 h on a scale with an error of no more than 0.1%. When weighing, the samples are pre-wiped with a wrung-out damp cloth. The mass of water flowing out of the pores of the sample on the scale cup is included in the mass of the saturated sample. The test is carried out until the results of two consecutive weight measurements differ by no more than 0.1%.

The water absorption of concrete of a separate sample W_m by weight as a percentage with an error of up to 0.1% is calculated by the formula:

$$W_m = \frac{m_s - m_w}{m_s} \cdot 100\%, \quad (11)$$

where m_c is the mass of the dried sample, [g], and m_w is the mass of the water-saturated sample, [g].

The water absorption of concrete of a separate sample W_0 by volume as a percentage with an error of up to 0.1% is calculated by the formula:

$$W_0 = \frac{W_m \cdot \rho_0}{\rho_w}, \quad (12)$$

where ρ_0 is the average density of dry concrete, [g/cm^3] and ρ_w is the density of water assumed to be equal to 1, [g/cm^3].

The total pore volume of V_p concrete is calculated as a percentage with an error of up to 0.1% according to the formula:

$$V_p = \frac{\rho - \rho_d}{\rho} \cdot 100\%, \quad (13)$$

where ρ is the true density of concrete, [kg/m^3] and ρ_d is the density of dried concrete, [kg/m^3].

The volume of open capillary pores of concrete (sample) V_o is assumed to be equal to the water absorption of concrete by volume W_0.

The volume of conditionally closed capillary pores of concrete V_c is calculated by the formula:

$$V_c = V_p - V_o. \quad (14)$$

2.4. Determination of the Compressive Strength of Cement Stone

The strength was determined using a hydraulic press P-50 on samples of cement stone with a face length of 10 cm. The working area of the press consists of two horizontal plates mounted on a column with a lead screw. During the compression test, the samples were installed on the lower base plate of the press centrally relative to its longitudinal axis.

After installing the test sample on the base plates of the press (additional steel plates), the upper plate was combined with the upper support face of the sample (additional steel plate) so that their planes were completely adjacent to each other. Then the loading began.

The loading of the samples was carried out continuously with a constant rate of increase of the load until their destruction. At the same time, the loading time of the test sample before its destruction was at least 30 s. The maximum force achieved during the test was taken as a destructive load.

The compressive strength of concrete R_c for each sample is calculated by the formula:

$$R_c = \alpha \frac{F}{A}, \quad (15)$$

where α is the scale factor for reducing the strength of concrete to the strength of concrete in samples of basic size and shape, assumed to be 0.95 according to GOST 10180-2012 «Concretes. Methods for strength determination using reference specimens» [67]; F is destructive load, [N]; A is the area of the working section of the sample, [mm^2].

2.5. Differential Thermal Analysis of Cement Stone

Differential thermal analysis (DTA) is a method of studying physical and chemical transformations accompanied by the release or absorption of heat. The method is used to

register phase transformations in a sample and study their parameters. The analysis was carried out according to the standard method on the Q-1500D derivatograph.

In preparation for the study, the cement stone is crushed to pieces of 1–3 mm in size. The weight of crushed cement stone weighing 1–2 g is transferred to the box, filled with 100% ethyl alcohol, and left for 10 h. To separate the material from alcohol, filtration is carried out through a paper filter. The dehydrated material is crushed in a mortar to powder. Then, 0.5–1 g is taken from the powdered material, which is placed in the crucible of the derivatograph.

At a heating rate of 10 °C/min and a temperature range of 20–1000 °C, the temperature curve and the mass loss curve of the substance are fixed. The analysis of the derivatograms was carried out according to the standard methodology.

2.6. Quantitative Analysis of Calcium Ions in a Liquid Medium by the Method of Complexometry

The complexometric determination of calcium cations is based on direct titration of the test solution with a standard solution of complexon III with the addition of indicators of murexide or dark blue chromogen. The indicators form a complex compound of red color with calcium ions. When titrating the test solution with complexon III at the equivalence point, the red color changes to the color characteristic of the free indicator.

A total of 25 mL of the analyzed solution is pipetted into a conical flask, and 50 mL of distilled water, 25 mL of a 20% sodium hydroxide solution, and 2–3 drops of the indicator are added to it. Then the test solution is titrated with a 0.1 N solution of complexon III with continuous stirring until the red color changes to purple or blue. In the end, titration is carried out very slowly.

The calculation of the content of calcium cations in the solution is carried out according to the formula:

$$g_A = \frac{E_A \cdot N_B \cdot V_B}{1000}, \tag{16}$$

where g_A is the total content of calcium cations in solution, [g]; E_A is the equivalent of calcium cations; N_B is the concentration of standard EDTA solution, [eq/L]; V_B is the volume of standard EDTA solution spent on titration, [mL].

2.7. Mathematical Model of the Second Type of Corrosion of Cement Concretes

When studying the II type of corrosion of cement concretes by our scientific school for the system under consideration, «cement stone–aggressive component», the mass transfer equations for calcium hydroxide are presented in the form of the following boundary value task [68]:

$$\frac{\partial C(x,\tau)}{\partial \tau} = k\frac{\partial^2 C(x,\tau)}{\partial x^2} + \frac{q_v(x)}{\rho_{con}},\ \tau \geq 0,\ 0 \leq x \leq \delta, \tag{17}$$

$$C(x,\tau)|_{\tau=0} = C_0(x), \tag{18}$$

$$\left.\frac{\partial C(x,\tau)}{\partial x}\right|_{x=0} = 0, \tag{19}$$

$$-k\rho \left.\frac{\partial C(x,\tau)}{\partial x}\right|_{x=\delta} = q_n. \tag{20}$$

where $C(x,\tau)$ is the concentration of «free calcium hydroxide» in concrete at time τ [s] at an arbitrary point with the x coordinate [m], in terms of CaO, [kg CaO/kg concrete]; k is the mass conductivity coefficient, [m^2/s]; $q_v(x)$ is the source of the mass of the substance as a result of a chemical reaction, [kg/(m^3·s)]; ρ_{con} is concrete density, [kg/m^3]; δ is the wall thickness of the structure, [m]; $C_0(x)$ is the concentration of «free calcium hydroxide» in concrete at the initial moment of time at an arbitrary point with the x coordinate, [kg CaO/kg concrete]; q_n is the density of the mass flow of a substance from concrete into a liquid medium, [kg/(m^2·s)].

The initial condition (Equation (18)) shows that at the time taken as the starting point, the concentration of the transferred component («free calcium hydroxide») has a distribution over the thickness of the concrete structure.

The boundary condition (Equation (19)) is a condition of non-penetration at the outer boundary of the structure.

The boundary condition (Equation (20)) is a condition of the second kind and shows that there is a mass transfer between the solid and liquid phases at the boundary of the structure with a liquid medium.

In the final form, the boundary value problem of mass conductivity in dimensionless variables is written:

$$\begin{aligned}\theta(\overline{x}, Fo_m) = &-\tfrac{Ki_m^*}{6}\left(6Fo_m + 3\overline{x}^2 - 1\right)\\ &+\tfrac{2Ki_m^*}{\pi^2}\sum_{n=1}^{\infty}\tfrac{(-1)^n}{n^2}\cos(\pi n\overline{x})\cdot exp\left(-\pi^2 n^2 Fo_m\right) + \int_0^1 \theta_0(\xi)d\xi\\ &+2\sum_{n=1}^{\infty}\cos(\pi n\overline{x})\int_0^1 \theta_0(\xi)\cos(\pi n\xi)d\xi\cdot exp\left(-\pi^2 n^2 Fo_m\right)\\ &+\left(Fo_m + \tfrac{3\overline{x}^2+2}{6}\right)\int_0^1 Po_m^*(\xi)d\xi\\ &-\int_0^1 Po_m^*(\xi)\cdot\xi\cdot d\xi + \tfrac{1}{2}\int_0^1 Po_m^*(\xi)\cdot\xi^2\cdot d\xi\\ &-\tfrac{2}{\pi^2}\sum_{n=1}^{\infty}\tfrac{1}{n^2}\cos(\pi n\overline{x})\int_0^1 Po_m^*(\xi)\cos(\pi n\xi)d\xi\\ &\cdot exp\left(-\pi^2 n^2 Fo_m\right),\end{aligned} \tag{21}$$

where $\theta(\overline{x}, Fo_m) = \frac{C(x,\tau)-C_0}{C_0}$ is the dimensionless concentration; $\overline{x} = \frac{x}{\delta}$ is the dimensionless coordinate; $Fo_m = \frac{k\tau}{\delta^2}$ is the Fourier mass transfer criterion; $Ki_m^* = \frac{q_n\delta}{kC_0\rho_{con}}$ is the modified Kirpichev criterion; n is the number of row members; ξ is the coordinate of integration in the range $0 \le \xi \le \overline{x}$; $Po^*(\overline{x}) = \frac{q_v(x)\delta^2}{kC_0\rho_{con}}$ is the modified Pomerantsev criterion.

3. Results and Discussion

Images of the cement stone surface (Figure 1) were obtained using a digital portable electron microscope USB Digital Microscope at a magnification of 50 times. The images show white crystals of calcium stearate in the pores and structure of cement stone. It can be noticed that with an increase in the concentration of the additive, the particle size becomes larger. Figure 1 shows that calcium stearate fills the pores, preventing the ingress of an aggressive environment deep into the cement stone. The study of the introduction of calcium stearate into the cement stone of concrete and aspects of pore colmatation can be carried out additionally and presented in subsequent publications.

During the setting period of the cement dough (from 0 to 2 h), moisture evaporation occurs faster in cement samples without additives than in hydrophobized ones (Figure 2). The beginning of the setting occurs after 1 h of holding the samples in the air and ends after 2 h from the moment of pouring into the mold. In samples containing calcium stearate additives, the onset of setting occurs after 2 h and ends 3 h after manufacture.

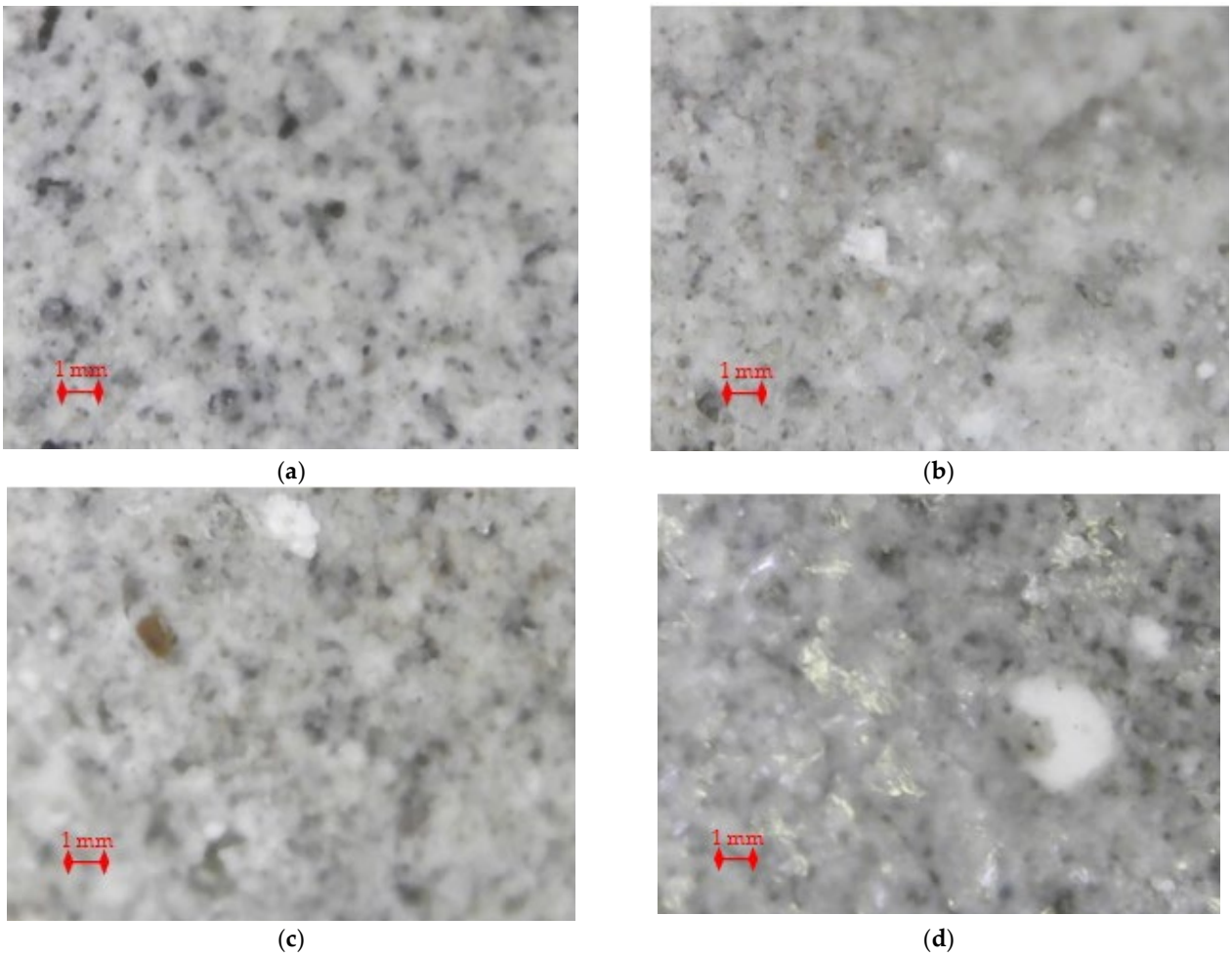


Figure 1. Images of the surface of concrete samples: (**a**) without calcium stearate; (**b**) the concentration of the hydrophobic additive is 0.8%; (**c**) the concentration of the hydrophobic additive is 1.1%; (**d**) the concentration of the hydrophobic additive is 1.3%.

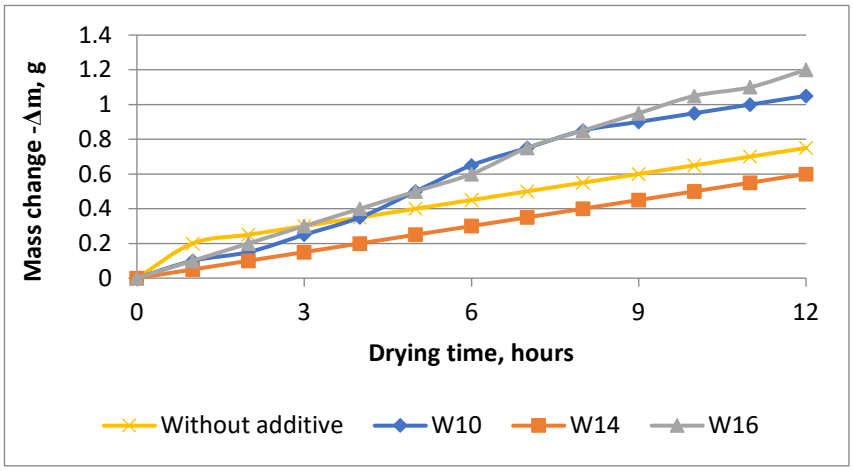


Figure 2. Change in the mass of cement stone samples with calcium stearate additives during the first 12 h of air hardening.

The results of the studies show that in samples with a concentration of calcium stearate of 1.1%, the mass change at the initial stage of hardening occurs uniformly. During the first 12 h, in samples with a hydrophobic additive content of 0.8% and 1.3%, the mass

change occurs most intensively, while the concentration of the additive in the amount of 1.1% does not significantly affect the change in the mass of the samples compared to the sample without additives.

A greater change in the mass of samples with the addition of 0.8% and 1.3% calcium stearate may be due to the fact that the particles of the hydrophobizer slow down the interaction of the cement mixture with water, as a result of which the water remains on the surface and does not settle but evaporates. The difference in the intensity of the change in the mass of cement stone samples with hydrophobic additives during hardening may be due to the different distribution of calcium stearate particles in the cement volume during mixing.

However, after a day, the trend of changing the mass of samples does not persist, as can be seen in Figure 3. With further hardening, cement stone without the addition of calcium stearate shows a greater change in mass due to drying and evaporation of moisture not only from the surface but also from the structure in the subsurface layer. In hydrophobized samples, water remains trapped inside the pores due to the distribution of hydrophobizer particles in the cement stone structure [69–71]. Evaporation of moisture, in this case, occurs only on the surface of the samples, and the processes of hydration of cement continue inside [72]. This leads to the formation of more calcium-containing phases in the structure of cement stone, in particular calcium hydrosilicates, which are carriers of the mechanical strength of concrete [70,73–75]. As a result, hydrophobic concrete has improved strength characteristics [40,46,76].

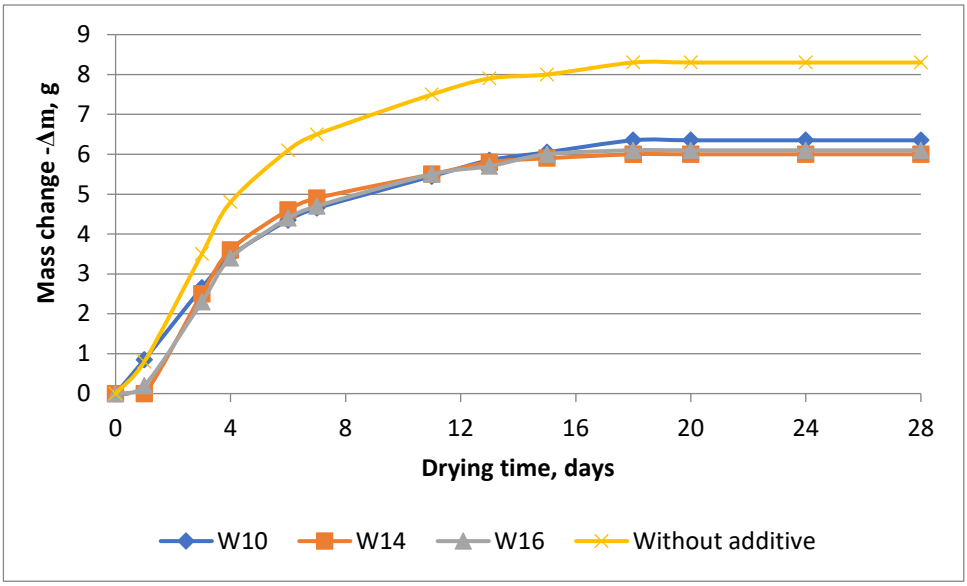


Figure 3. Change in the mass of cement stone samples with calcium stearate additives during air hardening at 20 °C.

Figure 3 shows that the change in the mass of cement stone samples with additives in the amount of 1.1% and 1.3% reaches constant values within 13–14 days; the samples showed the smallest change in mass during air hardening. In samples with a concentration of 0.8% calcium stearate additive, mass transfer processes slow down after 15 days of testing. Drying of the sample without additives takes place on the 18th day of exposure to air while achieving the maximum change in mass for the studied objects.

It is known that hydrophobic additives introduced into concrete at the manufacturing stage contribute to improving its operational characteristics [53–55,60]. The introduction of hydrophobic additives into the cement mixture reduces the amount of water evaporating during hardening, which leads to increased hydration processes and, as a consequence, changes in the characteristics of the cement stone of concrete (Table 3).

An increase in density due to a decrease in porosity should help slow down the penetration of an aggressive medium deep into the cement stone of concrete and inhibit the development of corrosion processes.

Determination of the kinetics of dissolution and leaching of calcium ions from cement stone by an aggressive chloride-containing medium was carried out when samples were immersed in a 2% $MgCl_2$ solution. The content of calcium cations in the liquid medium was determined by the method described in Section 2.6. During the tests, it was found that the state close to the equilibrium concentration of calcium cations in the solution is reached after 14 days of stay of hydrophobized cement stone samples in a corrosive environment (curves 2, 3, and 4 in Figure 4) [58,77], whereas, for samples without a hydrophobizing additive, the equilibrium state occurs after 150 days of testing (curve 1 on Figure 4).

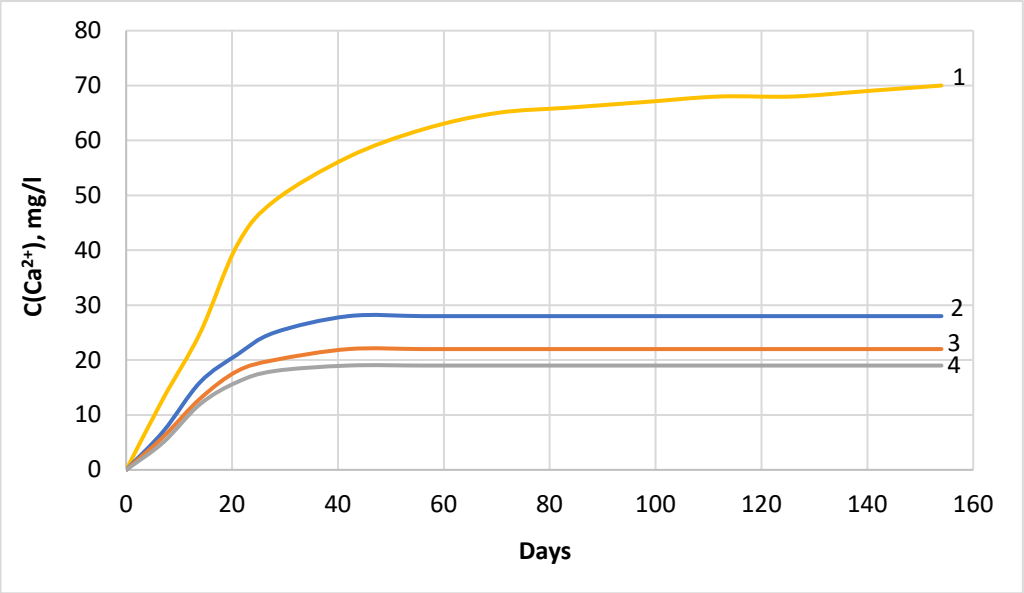


Figure 4. Kinetic curves of the concentration of calcium cations in a 2% $MgCl_2$ solution of cement stone samples: (1) non-hydrophobic; (2) waterproof grade W10; (3) waterproof grade W14; (4) waterproof grade W16.

It is obvious that for cement concrete containing 1.1 and 1.3% by weight of the hydrophobizer, the kinetics of calcium leaching in an aggressive environment is almost the same (curves 3 and 4 in Figure 4); therefore, further studies were carried out on the samples of the W10 and W16 waterproof grades.

With the help of a derivatographic analysis, the content of calcium hydroxide in different parts of the cement stone was determined, which made it possible to calculate and construct profiles of the concentrations of «free calcium hydroxide» according to the thickness of hydrophobized cement stone samples exposed to a 2% $MgCl_2$ solution at different stages of the experiment using the mathematical model (Equation (21)) (Figures 5 and 6).

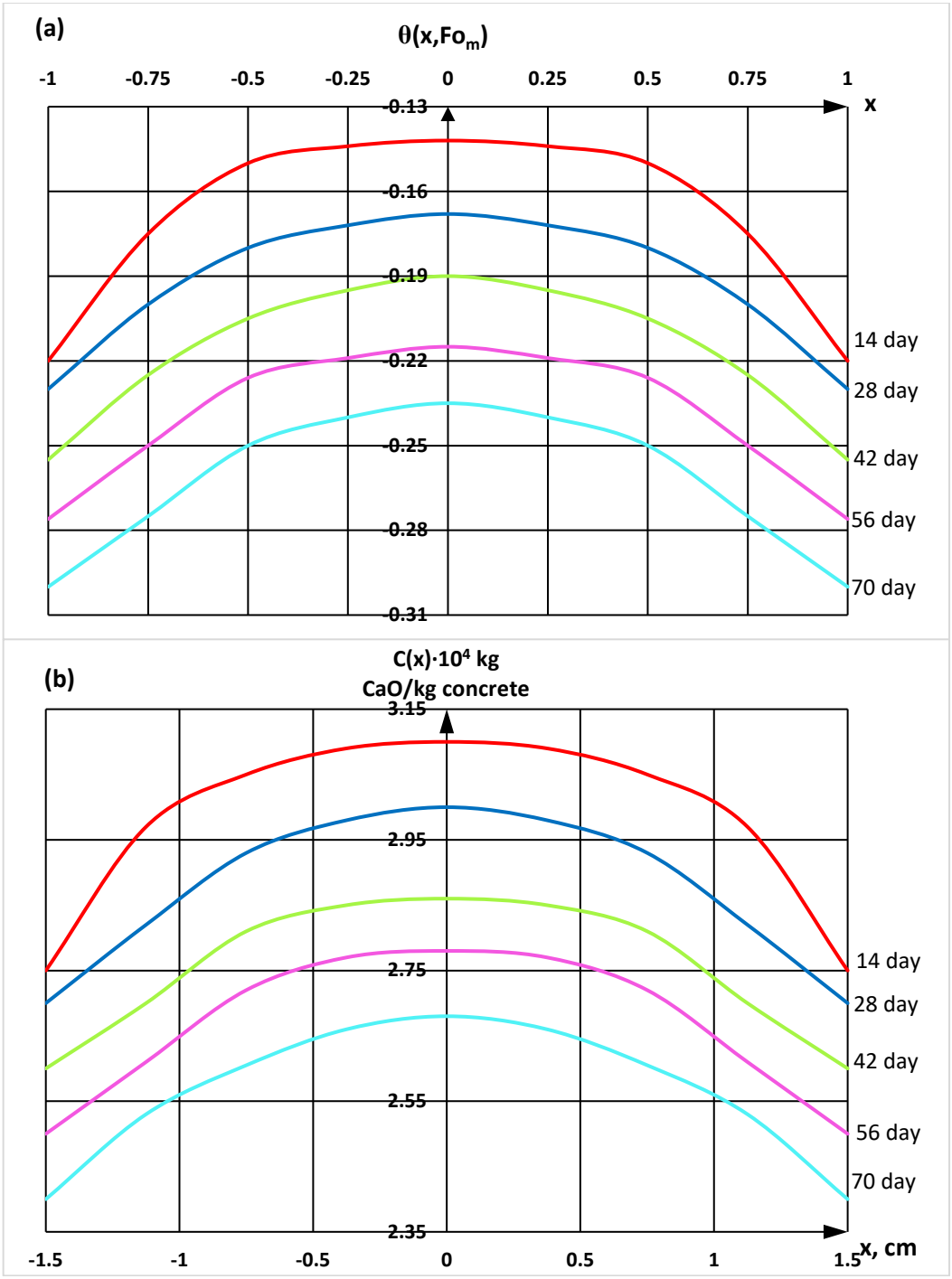


Figure 5. Profiles of concentrations of «free calcium hydroxide» by the thickness of the W10 waterproof grade sample in dimensionless coordinates (**a**) and in coordinates with real physical dimensions (**b**).

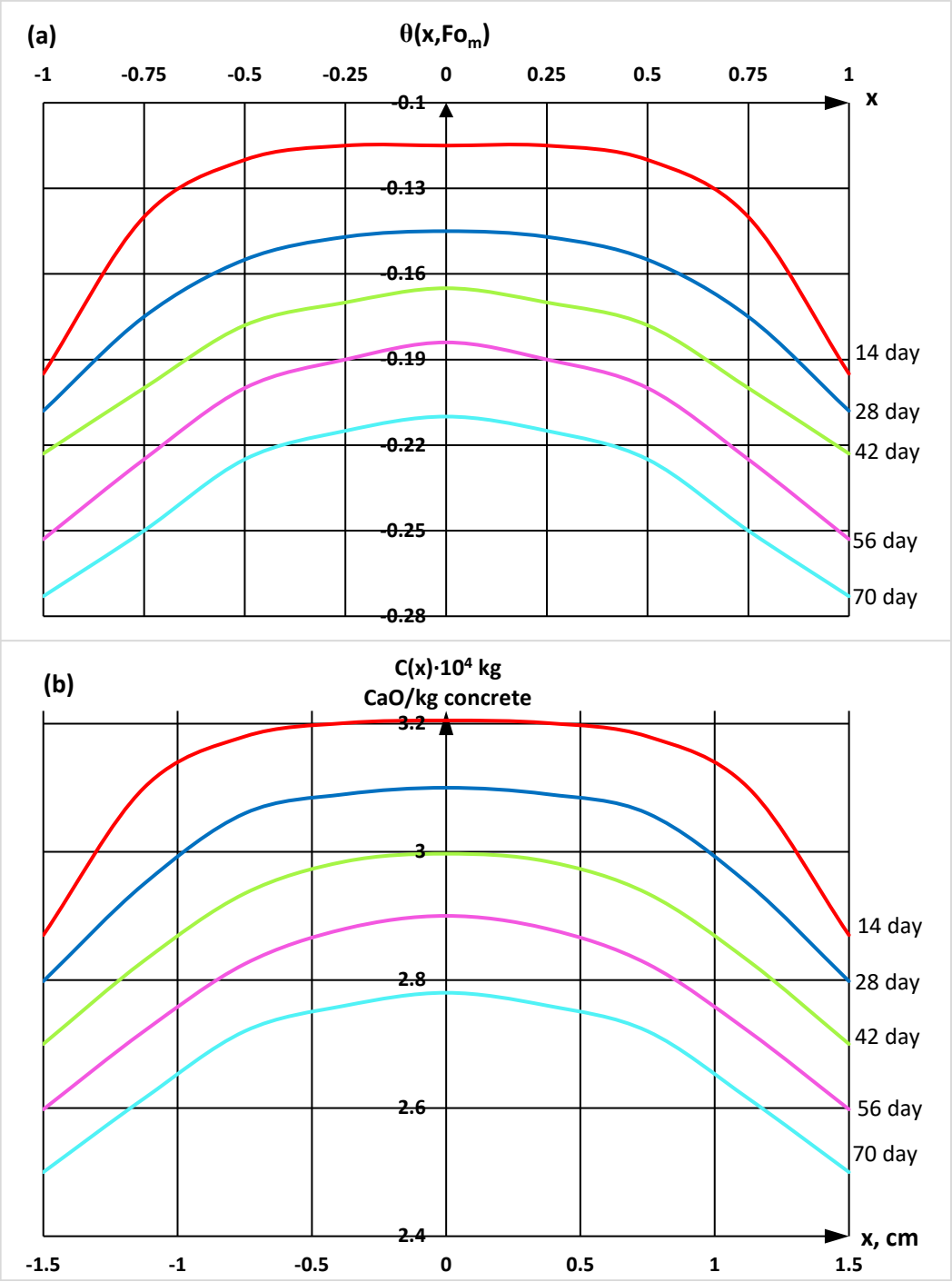


Figure 6. Profiles of concentrations of «free calcium hydroxide» by the thickness of the W16 waterproof grade sample in dimensionless coordinates (**a**) and in coordinates with real physical dimensions (**b**).

According to formulas (Equations (22) and (23)), the characteristics of the mass transfer process of "free calcium hydroxide" during the corrosion of hydrophobic concrete in 2% $MgCl_2$ solution were calculated (Figures 7 and 8).

$$k = \frac{q}{\rho_0 \frac{dC}{dx}}, \quad (22)$$

where k is the mass conductivity coefficient, [m^2/s]; q is the mass flow density due to chemical reactions, [kg/(m^2·s)]; ρ_0 is the density of the solid phase, [kg/m^3].

$$q = \frac{\Delta C_{liq}}{S \cdot \tau}, \tag{23}$$

where ΔC_{liq} is the mass of the substance transferred from the cement stone to the liquid medium, [kg]; S is the area of the corroded concrete surface, [m^2]; τ is the process time, [s].

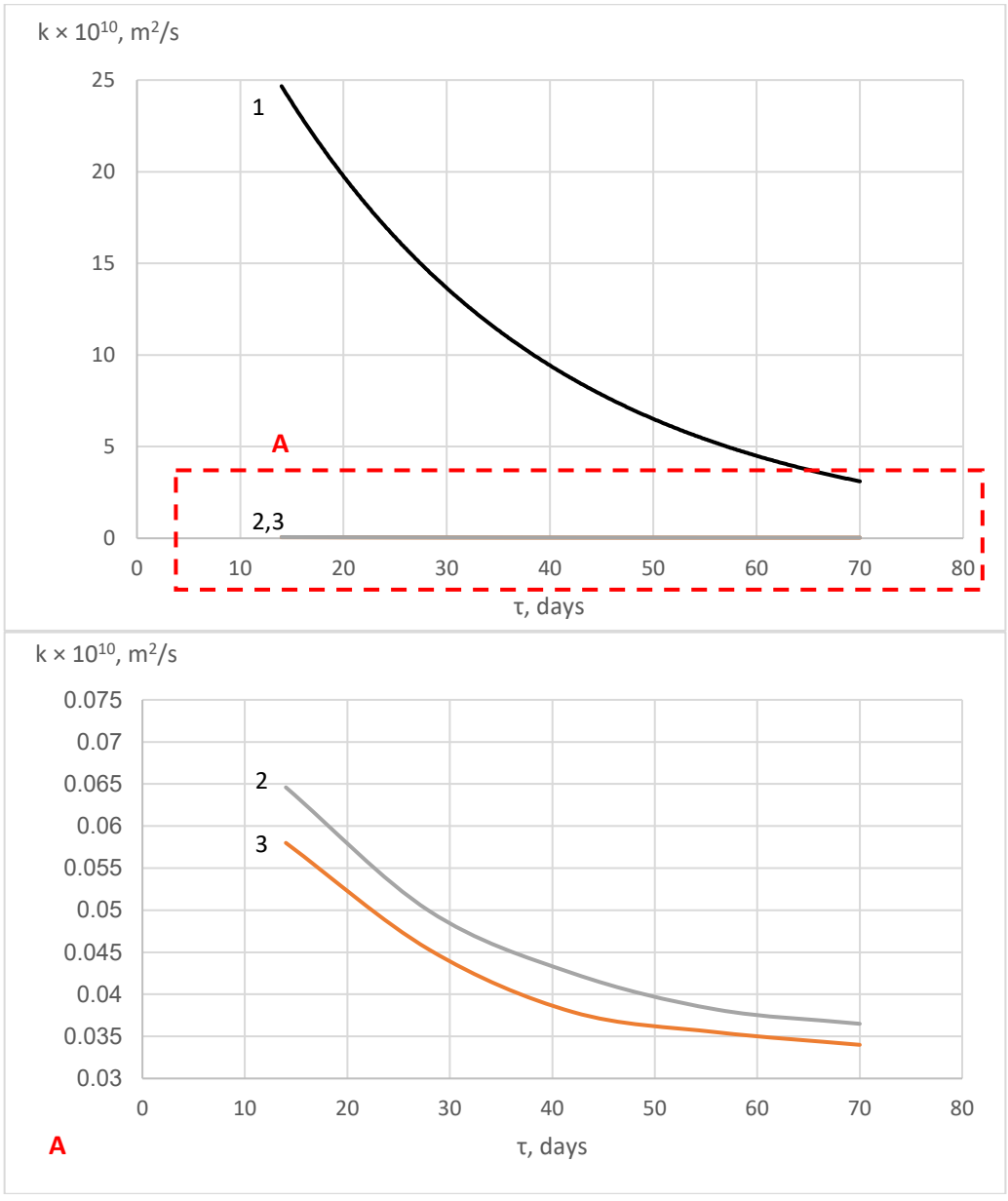


Figure 7. Change in the values of the mass conductivity coefficient during corrosion of cement stone samples in a 2% $MgCl_2$ solution: (1) sample without additive; (2) sample of the W10 waterproof grade; (3) sample of the W16 waterproof grade.

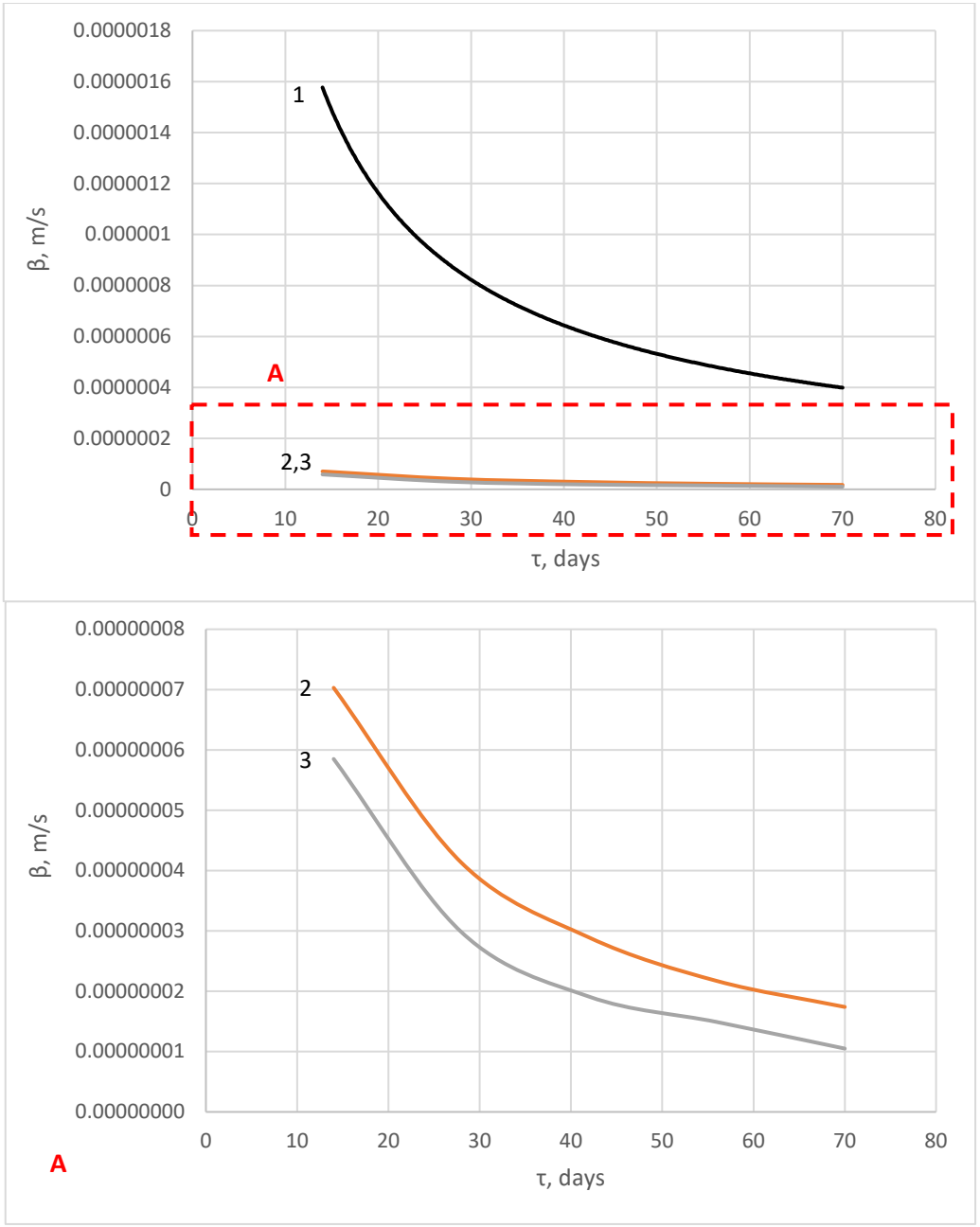


Figure 8. Change in the values of the mass transfer coefficient during corrosion of cement stone samples in a 2% $MgCl_2$ solution: (1) sample without additive; (2) sample of the W10 waterproof grade; (3) sample of the W16 waterproof grade.

To calculate the processes of substance transfer, it is convenient to enter the mass transfer coefficient β. It is defined as the ratio of the diffusion flux q to the concentration difference ΔC, [kg/m^3]:

$$\beta = \frac{q}{\Delta C}. \quad (24)$$

Figure 8 shows that the mass conductivity coefficient of hydrophobized cement stone samples under corrosion in a 2% $MgCl_2$ solution varies exponentially. The curves have a flatter appearance compared to the curve of a non-hydrophobized sample, which indicates a significantly lower rate of corrosion processes in this case. The mass transfer coefficients behave in a similar way (Figure 8).

The shape of the curves in Figures 7 and 8 (letter A) corresponds to the slowing down of mass transfer processes occurring in hydrophobized cement stone during liquid corrosion and is consistent with the kinetic curves shown in Figure 4. This behavior is caused by the inhibition of the dissolution of calcium-containing phases in cement stone under the influence of a liquid-aggressive medium [78] due to the complication of the penetration of chloride ions deep into the pore structure of cement stone due to the hydrophobicity of the pore surface and their colmatation with calcium stearate [58]. The values of the mass transfer coefficients corresponding to the equilibrium state are used to determine the terms of maintenance-free service life of the concrete and reinforced concrete products under the influence of liquid-aggressive media [79].

4. Conclusions

The processes of mass transfer and mass conductivity significantly slow down with an increase in the density of concrete. Consequently, due to the formation of a denser structure of cement stone, including through volumetric hydrophobization, the corrosion resistance of concrete in environments of varying degrees of aggressiveness increases.

In comparison with some other hydrophobic additives, calcium stearate does not hamper hydration processes during concrete hardening. The addition of stearate into the cement mixture in the manufacture of concrete contributes to an increase in strength due to the formation of a large number of calcium-containing phases in the structure due to a more complete interaction of cement components with non-evaporating water. Calcium stearate belongs to hazard class 3; that is, it is moderately dangerous. Since the concentration of additives in concrete does not exceed 1.5% by weight of cement, they have no impact on human health and the environment.

To ensure uniform volumetric hydrophobization of cement stone, it is necessary to introduce calcium stearate in powdered form followed by thorough mixing. The introduction of calcium stearate increases the density of concrete cement stone, as can be seen in Table 3, which makes it difficult to use it for the hydrophobization of light and air-entrained concretes.

The introduction of hydrophobic additives increases the service life of a concrete product in case of corrosion in a highly aggressive liquid chloride-containing medium by four times. Volumetric hydrophobization allows for reducing water absorption and increasing the density of cement stone, which means reducing the amount of aggressive medium entering the concrete and reducing the degree of corrosion destruction of cement stone. The conducted studies of the corrosion resistance of cement stone with hydrophobizing additives in a liquid chloride-containing medium using mathematical modeling allowed us to determine the parameters of mass transfer (coefficients of mass conductivity and mass transfer), which can be used to establish the terms of safe operation of concrete structures.

The paper defines the main parameters of corrosion mass transfer (coefficients of mass conductivity and mass transfer) for Portland cement of the CEM I 42.5 N brand with the addition of a calcium stearate hydrophobizer in a highly aggressive medium, which can be used to calculate the service life of concrete and reinforced concrete products using mathematical models of corrosion.

The obtained ideas about the corrosion destruction of hydrophobized concrete, taking into account the regularities of mass transfer processes, allow us to predict the effects of liquid media of varying degrees of aggressiveness on concrete and develop recommendations for improving the corrosion resistance of concrete and reinforced concrete products.

Funding: This research received no external funding.

Institutional Review Board Statement: Not applicable.

Informed Consent Statement: Not applicable.

Data Availability Statement: Data sharing is not applicable to this article.

Conflicts of Interest: The author declares no conflict of interest.

References

1. Jedidi, M.; Benjeddou, O. Chemical Causes of Concrete Degradation. *MOJ Civ. Eng.* **2018**, *4*, 00095. [CrossRef]
2. Bertolini, L.; Elsener, B.; Pedeferri, P.; Redaelli, E.; Polder, R.B. *Corrosion of Steel in Concrete: Prevention, Diagnosis, Repair*; Wiley-VCH Verlag GmbH & Co.: Weinheim, Germany, 2013; 434p.
3. Asamoto, S.; Sato, J.; Okazaki, S.; Chun, P.-J.; Sahamitmongkol, R.; Nguyen, G.H. The Cover Depth Effect on Corrosion-Induced Deterioration of Reinforced Concrete Focusing on Water Penetration: Field Survey and Laboratory Study. *Materials* **2021**, *14*, 3478. [CrossRef]
4. Fedosov, S.V.; Rumyantseva, V.E.; Krasilnikov, I.V.; Krasilnikova, I.A. Research of physical and chemical processes in the system "cement concrete—Liquid aggressive environment". *ChemChemTech* **2022**, *65*, 61–70.
5. Ortega, N.F.; Moro, J.M.; Meneses, R. Corrosion in Concrete Structures with Permanent Deformation in Marine Environment. *Open Constr. Build. Technol. J.* **2017**, *11*, 14–24. [CrossRef]
6. Claisse, P.A. *Transport Properties of Concrete: Modelling the Durability of Structures*, 2nd ed.; Woodhead Publishing: Sawston, UK, 2020; 328p.
7. Ding, X.; Liang, X.; Zhang, Y.; Fang, Y.; Zhou, J.; Kang, T. Capillary Water Absorption and Micro Pore Connectivity of Concrete with Fractal Analysis. *Crystals* **2020**, *10*, 892. [CrossRef]
8. Zhu, H.; Li, Q.; Ma, R.; Yang, L.; Hu, Y.; Zhang, J. Water-repellent additive that increases concrete cracking resistance in dry curing environments. *Constr. Build. Mater.* **2020**, *249*, 118704. [CrossRef]
9. Tuskaeva, Z.; Karyaev, S. Influence of various additives on properties of concrete. *E3S Web Conf.* **2020**, *164*, 14007. [CrossRef]
10. Okere, C.E.; Nwankwo, E.I.; Arinze, B.C.; Osukalu, E.J. Waterproof Concrete Additives and Their Effects on Concrete Properties. *J. Multidiscip. Eng. Sci. Technol. JMEST* **2017**, *4*, 7621–7623.
11. Tian, Y.; Wang, P.; Zhao, T.; Ma, Z.; Jin, Z.; Zhao, H. Influence of Water-Repellent Treatment with Silicon Resin on Properties of Concrete. *Adv. Mater. Sci. Eng.* **2019**, *2019*, 5743636. [CrossRef]
12. Ramachandran, V.S. *Concrete Admixtures Handbook. Properties, Science and Technology*; William Andrew: Norwich, NY, USA, 1996; 1184p.
13. Cappellesso, V.G.; dos Santos Petry, N.; Dal Molin, D.C.C.; Masuero, A.B. Use of crystalline waterproofing to reduce capillary porosity in concrete. *J. Build. Pathol. Rehabil.* **2016**, *1*, 9. [CrossRef]
14. Medeiros, M.H.F.; Castro-Borges, P.; Aleixo, D.M.; Quarcioni, V.A.; Marcondes, C.G.N.; Helene, P. Reducing Water and Chloride Penetration Through Silicate Treatments for Concrete as a Mean to Control Corrosion Kinetics. *Int. J. Electrochem. Sci.* **2012**, *7*, 9682–9696.
15. Jaskulski, R.; Jóźwiak-Niedźwiedzka, D.; Yakymechko, Y. Calcined Clay as Supplementary Cementitious Material. *Materials* **2020**, *13*, 4734. [CrossRef]
16. Singh, N.B. Clays and Clay Minerals in the Construction Industry. *Minerals* **2022**, *12*, 301. [CrossRef]
17. Geng, Y.; Li, S.; Hou, D.; Chen, X.; Jin, Z. Effect of SiO_2 Sol/Silane Emulsion in Reducing Water and Chloride Ion Penetration in Concrete. *Coatings* **2020**, *10*, 682. [CrossRef]
18. Ayad, A.; Said, A. Using Colloidal Nano Silica to Enhance the Performance of Cementitious Mortars. *Open J. Civ. Eng.* **2018**, *8*, 82–90. [CrossRef]
19. Breilly, D.; Fadlallah, S.; Froidevaux, V.; Colas, A.; Allais, F. Origin and industrial applications of lignosulfonates with a focus on their use as superplasticizers in concrete. *Constr. Build. Mater.* **2021**, *301*, 124065. [CrossRef]
20. Dvorkin, L.I. The influence of polyfunctional modifier additives on properties of cement-ash fine-grained concrete. *Mag. Civ. Eng.* **2020**, *93*, 121–133.
21. Qin, Y.L.; Bai, M.X.; Zhang, Z.M.; Yang, D.J. Adsorption Behavior of Naphthalene Sulfonate Formaldehyde Condensate with Different Molecular Weights on the Cement Particle Surface. *Adv. Mater. Res.* **2012**, *557–559*, 870–876. [CrossRef]
22. Khudhair, M.H.R.; Elyoubi, M.S.; Elharfi, A. Study of the influence of water reducing and setting retarder admixtures of polycarboxylate «superplasticizers» on physical and mechanical properties of mortar and concrete. *J. Mater. Environ. Sci.* **2018**, *9*, 56–65.
23. Ramachandran, V.S.; Lowery, M.S.; Malhotra, V.M. Behaviour of ASTM Type V cement hydrated in the presence of sulfonated melamine formaldehyde. *Mater. Struct.* **1995**, *28*, 133–138. [CrossRef]
24. Paktiawal, A.; Alam, M. Effect of polycarboxylate ether-based superplasticizer dosage on fresh and hardened properties of cement concrete. *IOP Conf. Ser. Mater. Sci. Eng.* **2021**, *1166*, 012013. [CrossRef]
25. Masanaga, M.; Hirata, T.; Kawakami, H.; Morinaga, Y.; Nawa, T.; Elakneswaran, Y. Effects of a New Type of Shrinkage-Reducing Agent on Concrete Properties. *Materials* **2020**, *13*, 3018. [CrossRef]
26. Özen, S.; Gökhan Altun, M.; Mardani-Aghabaglou, A. Effect of the polycarboxylate based water reducing admixture structure on self-compacting concrete properties: Main chain length. *Constr. Build. Mater.* **2020**, *255*, 119360. [CrossRef]
27. Li, W.; Wittmann, F.H.; Jiang, R.; Zhao, T.; Wolfseher, R. Integral Water Repellent Concrete Produced by Addition of Metal Soaps. *Restor. Build. Monum.* **2012**, *18*, 41–48. [CrossRef]
28. Misnikov, O.S.; Chertkova, E.Y. Hydrophobic modification of mineral binders by additives produced from peat. *Eurasian Min.* **2014**, *1*, 63–68.
29. Badikova, A.D.; Sakhibgareev, S.R.; Fedina, R.A.; Rakhimov, M.N.; Tsadkin, M.A. Effective mineral additive on the basis of wastes of petrochemical plants for a concrete structural mix. *Nanotechnol. Constr.* **2020**, *12*, 34–40. [CrossRef]

30. Teshaboeva, N.D. Basic issues of the theory of hydrophobization of cement systems by additives of products of petrochemical synthesis. *Orient. Renaiss. Innov. Educ. Nat. Soc. Sci.* **2021**, *1*, 475–479.
31. Albayrak, A.T.; Yasar, M.; Gurkaynak, M.A.; Gurgey, I. Investigation of the effects of fatty acids on the compressive strength of the concrete and the grindability of the cement. *Cem. Concr. Res.* **2005**, *35*, 400–404. [CrossRef]
32. Nemati Chari, M.; Naseroleslami, R.; Shekarchi, M. The impact of calcium stearate on characteristics of concrete. *Asian J. Civ. Eng.* **2019**, *20*, 1007–1020. [CrossRef]
33. Lanzón, M.; Martínez, E.; Mestre, M.; Madrid, J.A. Use of zinc stearate to produce highly-hydrophobic adobe materials with extended durability to water and acid-rain. *Constr. Build. Mater.* **2017**, *139*, 114–122. [CrossRef]
34. Ogurtsova, Y.N.; Strokova, V.V.; Labuzova, M.V. Hydrophobization of Concrete Using Granular Nanostructured Aggregate. *IOP Conf. Ser. Mater. Sci. Eng.* **2017**, *262*, 012013. [CrossRef]
35. Maryoto, A.; Setijadi, R.; Widyaningrum, A.; Waluyo, S. Drying Shrinkage of Concrete Containing Calcium Stearate, ($Ca(C_{18}H_{35}O_2)_2$), with Ordinary Portland Cement (OPC) as a Binder: Experimental and Modelling Studies. *Molecules* **2020**, *25*, 4880. [CrossRef]
36. Cellat, K.; Tezcan, F.; Kardaş, G.; Paksoy, H. Comprehensive investigation of butyl stearate as a multifunctional smart concrete additive for energy-efficient buildings. *Int. J. Energy Res.* **2019**, *43*, 7146–7158. [CrossRef]
37. Kurdi, A.; Almoatham, N.; Mirza, M.; Ballweg, T.; Alkahlan, B. Potential Phase Change Materials in Building Wall Construction—A Review. *Materials* **2021**, *14*, 5328. [CrossRef]
38. Liu, X.; Song, X.; Wang, Z.; Xia, C.; Li, T.; Li, X.; Xu, Q.; Cui, S.; Qian, S. Polymer for Internal Hydrophobization of Cement-Based Materials: Design, Synthesis, and Properties. *Polymers* **2021**, *13*, 3069. [CrossRef]
39. Luginina, A.A.; Kuznetsov, S.V.; Voronov, V.V.; Yapryntsev, A.D.; Ivanov, V.K.; Petukhov, D.I.; Lyapin, A.A.; Ermakov, A.S.; Pominova, D.V.; Chernova, E.V.; et al. Hydrophobization of up-conversion luminescent films based on nanocellulose/MF2:Ho particles (M = Sr, Ca) by acrylic resin. *Nanosyst. Phys. Chem. Math.* **2019**, *10*, 585–598. [CrossRef]
40. Sharma, N.; Sharma, P. Effect of hydrophobic agent in cement and concrete: A Review. *IOP Conf. Ser. Mater. Sci. Eng.* **2021**, *1116*, 012175. [CrossRef]
41. Sanjay Kumar, R.; Selvaraj, R.; Kumutha, R. Development of Superhydrophobic Coatings on Concrete Surfaces. *Int. J. Sci. Res. (IJSR)* **2017**, *6*, 363–368.
42. Zhang, P.; Shang, H.; Hou, D.; Guo, S.; Zhao, T. The Effect of Water Repellent Surface Impregnation on Durability of Cement-Based Materials. *Adv. Mater. Sci. Eng.* **2017**, *2017*, 8260103. [CrossRef]
43. Butakova, M.D.; Saribekyan, S.S.; Mikhaylov, A.V. Influence of Silicon-Containing Additives on Concrete Waterproofness Property. *IOP Conf. Ser. Mater. Sci. Eng.* **2017**, *262*, 012006. [CrossRef]
44. Grabowska, K.; Koniorczyk, M. Internal hydrophobization of cement mortar by addition of siloxanes. *MATEC Web Conf.* **2019**, *282*, 02030. [CrossRef]
45. Medeiros, M.; Helene, P. Efficacy of surface hydrophobic agents in reducing water and chloride ion penetration in concrete. *Mater. Struct.* **2008**, *41*, 59–71. [CrossRef]
46. Maryoto, A.; Sthenly Gan, B.; Intang Setyo Hermanto, N.; Setijadi, R. Effect of Calcium Stearate in the Mechanical and Physical Properties of Concrete with PCC and Fly Ash as Binders. *Materials* **2020**, *13*, 1394. [CrossRef]
47. Azad, A.; Mousavi, S.F.; Karami, H.; Farzin, S. Application of Talc as an Eco-Friendly Additive to Improve the Structural Behavior of Porous Concrete. *Iran. J. Sci. Technol. Trans. Civ. Eng.* **2019**, *43*, 443–453. [CrossRef]
48. Lima-Guerra, D.J.; Mello, I.; Resende, R.; Silva, R. Use of Bentonite and Organobentonite as Alternatives of Partial Substitution of Cement in Concrete Manufacturing. *Int. J. Concr. Struct. Mater.* **2014**, *8*, 15–26. [CrossRef]
49. Raheem, S.A.; Saheb, M.A.; Moula, H.H.; Maula, B.H.; Alshreefi, R.A.; Bahnam, Q.M. Improve Light Weight Concrete Characteristics by Adding Paraffin Wax as Moisture Proof. *Mater. Sci. Forum* **2019**, *972*, 16–25. [CrossRef]
50. Li, Z.; Sun, W.; Liu, S.; Li, Z.; Deng, B.; Wu, J.; Ding, Y.; Jiao, K.; Jin, X.; Lu, P.; et al. Pore Preservation and Failure Mechanism of Sinian Dengying Formation Carbonate Reservoirs: A Case Study of Two Ultradeep Wells in the Sichuan Basin, Western China. *Geofluids* **2021**, *2021*, 8387748. [CrossRef]
51. Anikina, N.A.; Smirnov, V.F.; Smirnova, O.N.; Zaharova, E.A. Protection of construction materials based on acrylates from biodeterioration. *Mag. Civ. Eng.* **2018**, *81*, 116–124.
52. Yao, S.Y.; Ge, Y. Effect of Styrene Butadiene Rubber Latex on Mortar and Concrete Properties. *Adv. Eng. Forum* **2012**, *5*, 283–288. [CrossRef]
53. Abdo, S.; Galishnikova, V.V.; Fawzy, A.M. Properties of recycled aggregate pervious concrete modified with Styrene Butadiene Rubber Latex. *Mag. Civ. Eng.* **2021**, *108*, 10805.
54. Kim, M.J.; Park, E.S.; Hwang, W.I.; Cho, W.J. Effect of FNS Incorporation on the Properties of Ternary Blended Cement Containing Blast Furnace Slag and Fly Ash. *Adv. Mater. Sci. Eng.* **2022**, *2022*, 1047648. [CrossRef]
55. Sychova, A.M.; Svatovskaya, L.B.; Starchukov, D.S.; Soloviova, V.Y.; Gravit, M.V. The improving of the concrete quality in a monolithic clip. *Mag. Civ. Eng.* **2018**, *80*, 3–14.
56. Cardenas, H.; Kupwade-Patil, K.; Eklund, S. Corrosion Mitigation in Mature Reinforced Concrete Using Nanoscale Pozzolan Deposition. *J. Mater. Civ. Eng.* **2011**, *23*, 752–760. [CrossRef]

57. de Souza Oliveira, A.; Gomes, O.F.M.; Ferrara, L.; Fairbairn, E.M.R.; Filho, R.D.T. An overview of a twofold effect of crystalline admixtures in cement-based materials: From permeability-reducers to self-healing stimulators. *J. Build. Eng.* **2021**, *41*, 102400. [CrossRef]
58. Fedosov, S.V.; Roumyantseva, V.E.; Krasilnikov, I.V.; Konovalova, V.S.; Evsyakov, A.S. Monitoring of the Penetration of Chloride Ions to the Reinforcement Surface through a Concrete Coating during Liquid Corrosion. *IOP Conf. Ser. Mater. Sci. Eng.* **2018**, *463*, 042048. [CrossRef]
59. Basheer, P.A.M.; Basheer, L.; Cleland, D.J.; Long, A.E. Surface Treatments for Concrete: Assessment Methods and Reported Performance. *Constr. Build. Mater.* **1997**, *11*, 413–429. [CrossRef]
60. Suchorab, Z.; Barnat-Hunek, D.; Franus, M.; Łagód, G. Mechanical and Physical Properties of Hydrophobized Lightweight Aggregate Concrete with Sewage Sludge. *Materials* **2016**, *9*, 317. [CrossRef]
61. Zhu, H.; Wang, P.; Zhang, G. Effect of hydrophobic agent on efflorescence of portland cement-based decorative mortar. *Jianzhu Cailiao Xuebao/J. Build. Mater.* **2014**, *17*, 882–886.
62. Pasupathy, K.; Ramakrishnan, S.; Sanjayan, J. Effect of hydrophobic surface-modified fine aggregates on efflorescence control in geopolymer. *Cem. Concr. Compos.* **2022**, *126*, 104337. [CrossRef]
63. Mussato, B.T.; Gepraegs, O.K.; Farnden, G. Relative Effects of Sodium Chloride and Magnesium Chloride on Reinforced Concrete: The State of Art. *Transp. Res. Rec. J. Transp. Res. Board* **2004**, *1866*, 59–66. [CrossRef]
64. Markov, A.I. Way Determining Waterproofness of Cement Materials. Patent RU2187804, 20 August 2002.
65. *MI 2625-2000*; Recommended Practice. National Measurement Standards. Cement Materials. Accelerated Method for Measuring Water Impermeability. VNIIFTRI GP: Moscow, Russia, 2000.
66. *GOST 12730.5-2018*; Concretes. Methods for determination of water tightness. Standartinform: Moscow, Russia, 2018.
67. *GOST 10180-2012*; Concretes. Methods for strength determination using reference specimens. Standartinform: Moscow, Russia, 2012.
68. Fedosov, S.V.; Roumyantseva, V.E.; Krasilnikov, I.V.; Konovalova, V.S. Physical and mathematical modelling of the mass transfer process in heterogeneous systems under corrosion destruction of reinforced concrete structures. *IOP Conf. Ser. Mater. Sci. Eng.* **2018**, *456*, 012039. [CrossRef]
69. Fic, S.; Szewczak, A.; Barnat-Hunek, D.; Łagód, G. Processes of Fatigue Destruction in Nanopolymer-Hydrophobised Ceramic Bricks. *Materials* **2017**, *10*, 44. [CrossRef]
70. Tsoy, V.M.; Turgayev, J.A.; Narbaev, U.I. Studying the structure and properties of cement stone with a complex of modifying additives. *ISJ Theor. Appl. Sci.* **2023**, *2*, 281–288. [CrossRef]
71. Al-Kheetan, M.J.; Rahman, M.M.; Chamberlain, D.A. Development of hydrophobic concrete by adding dual-crystalline admixture at mixing stage. *Struct. Concr.* **2018**, *19*, 1504–1511. [CrossRef]
72. Klisińska-Kopacz, A.; Tišlova, R. Effect of hydrophobization treatment on the hydration of repair Roman cement mortars. *Constr. Build. Mater.* **2012**, *35*, 735–740. [CrossRef]
73. Bogdanov, R.R.; Ibragimov, R.A. Process of hydration and structure formation of the modified self-compacting concrete. *Mag. Civ. Eng.* **2017**, *5*, 14–24.
74. Zhang, H.; Zhou, Y.; Mu, S.; Cai, J.; Hong, J.; Liu, J.; Zhao, Y. Pore Structure and Permeability of Cementitious Materials Containing a Carboxylic Acid Type Hydrophobic Agent. *Front. Mater.* **2022**, *9*, 907638. [CrossRef]
75. Trofimova, I.; Shpyrko, N. Investigating the influence of volumetric hydrophobization on the formation of phase composition of cement stone and its physical-mechanical properties. *East.-Eur. J. Enterp. Technol.* **2019**, *4*, 32–38. [CrossRef]
76. Tkacha, E.V.; Semenova, V.S.; Tkacha, S.A.; Rozovskayaa, T.A. Highly effective water-repellent concrete with improved physical and technical properties. *Procedía Eng.* **2015**, *111*, 763–769. [CrossRef]
77. Fedosov, S.V.; Roumyantseva, V.E.; Konovalova, V.S.; Evsyakov, A.S. The role of colmatation in liquid corrosion of hydrophobized concrete. *IOP Conf. Ser. Mater. Sci. Eng.* **2020**, *896*, 012096. [CrossRef]
78. Rumyantseva, V.E.; Konovalova, V.S.; Narmaniya, B.E. Changes in the structural and phase composition and strength characteristics of concrete during liquid corrosion in chloride-containing media. *J. Phys. Conf. Ser.* **2021**, *1926*, 012057. [CrossRef]
79. Fedosov, S.V.; Rumyantseva, V.E.; Krasilnikov, I.V.; Konovalova, V.S.; Karavaev, I.V. Determination of safe service life of structures made of concrete containing hydrophobic additives. *Izv. Vyss. Uchebnykh Zaved. Seriya Teknol. Tekst. Promyshlennosti* **2017**, *6*, 268–276.

Disclaimer/Publisher's Note: The statements, opinions and data contained in all publications are solely those of the individual author(s) and contributor(s) and not of MDPI and/or the editor(s). MDPI and/or the editor(s) disclaim responsibility for any injury to people or property resulting from any ideas, methods, instructions or products referred to in the content.